Simplified formulae for the estimation of the positive-sequence resistance and reactance of three-phase cables for different frequencies

Silva, Filipe Miguel Faria da

Published in:
Proceedings of the 2015 50th International Universities Power Engineering Conference (UPEC)

DOI (link to publication from Publisher):
10.1109/UPEC.2015.7339941

Publication date:
2015

Document Version
Accepted author manuscript, peer reviewed version

Simplified formulae for the estimation of the positive-sequence resistance and reactance of three-phase cables for different frequencies

F. Faria da Silva
Aalborg University – Department of Energy Technology, Denmark
ffs@et.aau.dk

***Abstract*-The installation of HVAC underground cables became more common in recent years, a trend expected to continue in the future. Underground cables are more complex than overhead lines and the calculation of their resistance and reactance can be challenging and time consuming for frequencies that are not power frequency.**

Software packages capable of performing exact calculations of these two parameters exist, but simple equations able to estimate the reactance and resistance of an underground cable for the frequencies associated to a transient or a resonance phenomenon would be helpful. This paper proposes new simplified formulae capable of calculating the positive-sequence resistance and reactance of a cable for frequencies associated to temporary overvoltages, slow-front overvoltages and resonance phenomena.

The calculation of a cable's resistance and reactance is made using a simplified series impedance matrix. The proposed formulae are validated by means of sensitivity tests and comparisons with generic cables. The paper finishes with an example demonstrating the estimation of the resonance frequency associated to a cable energisation using the formulae previously developed.

***Index Terms*—Underground Cables, Electromagnetic Transient, Inductance, Resistance, Resonance**

I. Nomenclature

A: impedance of the conductor-ground loop
B: mutual impedance between the conductor-ground and the screen-ground loops
C: impedance of the screen-ground loop
D: mutual impedance between cables
Z_{Couter}: conductor outer series impedance
$Z_{CSinsul}$: main insulation series impedance
Z_{Sinner}: screen inner-series impedance
Z_{Souter}: screen outer-series impedance
$Z_{SEinsul}$: outer insulation series impedances
$Z_{Smutual}$: mutual impedance of two loops
Z_{Earth}: earth-return impedance
Z_{Earth_mutual}: mutual impedance between cables
R_1: radius over the conductor
R_2: radius over the insulation
R_3: radius over the screen
R_4: outer radius of the cable
μ_C: permeability of the conductor
μ_S: permeability of the screen
ρ_C: conductor resistivity
ρ_S: screen resistivity
ρ_E: earth resistivity
$h_{i,j}$; depth of the cable conductor
d_{ij}: distance between two conductors
CS: cross-section area of the conductor
Z^+_{Re} : Positive-sequence resistance
Z^+_{Im} : Positive-sequence reactance
Z^+: Positive-sequence impedance
Z_{Ph}: Phase impedance
Z_{Seq}: Sequence impedance
l: length of the cable
C_{ap}: cable capacitance per unit of length
$L(f)$: cable inductance per unit of length in function of frequency
L_{eq}: inductance of the equivalent network

F. Faria da Silva is with Institute of Energy Technology, Aalborg University, 9220 Aalborg, Denmark (e-mail: ffs@et.aau.dk).

II. Introduction

The author proposed in [1] formulae that simplified the loop impedances of three-phase single-core cables. These formulae are used in this paper to develop simplified expressions able to estimate the positive-sequence resistance and reactance of the cables. The new proposed equations have a complexity level alike the formulae used for estimating these parameters at power frequency, but are also able to correctly estimate these two quantities for a large range of frequencies.

III. Positive-sequence impedance

The impedance matrix of a three-phase single-core cable is a 6x6 matrix [3], [4], which can be simplified to (1) for trefoil formations.

$$[Z]=\begin{bmatrix} A & B & D & D & D & D \\ B & C & D & D & D & D \\ D & D & A & B & D & D \\ D & D & B & C & D & D \\ D & D & D & D & A & B \\ D & D & D & D & B & C \end{bmatrix} \quad (1)$$

$$\begin{aligned} A &= Z_{Couter} + Z_{CSinsul} + Z_{Sinner} + Z_{Souter} + Z_{SEinsul} + Z_{Earth} - 2Z_{Smutual} \\ B &= Z_{Souter} + Z_{SEinsul} + Z_{Earth} - Z_{Smutual} \\ C &= Z_{Souter} + Z_{SEinsul} + Z_{Earth} \\ D &= Z_{Earth\_mutual} \end{aligned}$$

The positive-sequence impedance of (1) is calculated by re-arranging the matrix (2), where Z_{CoCo}, Z_{CoSc}, Z_{CoSc} and Z_{ScSc} are 3x3 sub-matrices. The values are transposed from the modal domain to the phase domain in (3) [6]. The positive, negative and zero-sequences are obtained using the Fortescue matrix (4), where (5) is the positive-sequence impedance of the conductor.

$$[Z] = \begin{bmatrix} A & D & D & B & D & D \\ D & A & D & D & B & D \\ D & D & A & D & D & B \\ B & D & D & C & D & D \\ D & B & D & D & C & D \\ D & D & B & D & D & C \end{bmatrix} \Leftrightarrow [Z] = \begin{bmatrix} Z_{CoCo} & Z_{CoSc} \\ Z_{CoSc} & Z_{ScSc} \end{bmatrix} \tag{2}$$

$$Z_{Ph} = Z_{CoCo} - Z_{CoSc} \cdot Z_{ScSc}{}^{-1} \cdot Z_{CoSc} \tag{3}$$

$$Z_{Seq} = H^{-1} \cdot Z_{Ph} \cdot H \tag{4}$$

$$Z^{+} = \frac{B^2 - 2BD - AC + AD + CD}{D - C} \tag{5}$$

Equation (5) can be rewritten as (6), which becomes (7) when the variables are separated into real and imaginary parts.

$$Z^{+} = A - D - \frac{(B-D)^2}{C-D} \tag{6}$$

$$Z^{+} = A_{\mathrm{Re}} + jA_{Im} - D_{\mathrm{Re}} - jD_{\mathrm{Im}} - \frac{\left(B_{Re} + jB_{im} - D_{\mathrm{Re}} - jD_{\mathrm{Im}}\right)^2}{C_{\mathrm{Re}} + jC_{\mathrm{Im}} - D_{\mathrm{Re}} - jD_{\mathrm{Im}}} \tag{7}$$

Equation (7) is divided into two, a real part corresponding to the resistance (8) and an imaginary part corresponding to the reactance (9). The real parts of variables B and D are alike, allowing further simplifications.

$$Z_{\mathrm{Re}}^{+} = A_{\mathrm{Re}} - D_{\mathrm{Re}} - \frac{\left(B_{\mathrm{Im}} - D_{\mathrm{Im}}\right)^2 \cdot \left(B_{Re} - C_{\mathrm{Re}}\right)}{\left(C_{\mathrm{Im}} - D_{\mathrm{Im}}\right)^2 + \left(C_{\mathrm{Re}} - D_{\mathrm{Re}}\right)^2} \tag{8}$$

$$Z_{\mathrm{Im}}^{+} = A_{Im} - D_{\mathrm{Im}} - \frac{\left(B_{\mathrm{Im}} - D_{\mathrm{Im}}\right)^2 \cdot \left(C_{\mathrm{Im}} - D_{\mathrm{Im}}\right)}{\left(C_{\mathrm{Im}} - D_{\mathrm{Im}}\right)^2 + \left(C_{\mathrm{Re}} - D_{\mathrm{Re}}\right)^2} \tag{9}$$

IV. Reactance and Resistance

A. Reactance

The reactance (10) is calculated substituting the variables in (9) by the equations from [1]. Notice that X has an extra simplification for R_2 and R_3, explained in [1].

$$Z_{\mathrm{Im}}^{+} = \frac{\sqrt{\omega \cdot \mu_0 \cdot \rho_c}}{\sqrt{8}\pi R_1} + \frac{\omega \cdot \mu_0}{2\pi} \ln\left(\frac{d_{ij} \cdot R_2}{R_1 \cdot R_3}\right) + \frac{8\omega \cdot \mu_0 \left(R_3 - R_2\right)}{6\pi\left(R_3 + R_2\right)} - \frac{\left(1.5X + Y\right)^2 \left(X + Y\right)}{\left(X+Y\right)^2 + \left(\frac{\rho_S}{\pi\left(R_3^2 - R_2^2\right)}\right)^2} \tag{10}$$

where, $X = \dfrac{\omega \cdot \mu_0 \left(R_3 - R_2\right)}{6\pi R_3}$ and $Y = \dfrac{\omega \cdot \mu_0}{2\pi} \ln\left(\dfrac{d_{ij}}{R_3}\right)$

The variable X is several times smaller than the variable Y, for typical cables. As a result, X may be removed and (10) simplifies to (11).

$$\begin{cases} Z_{\mathrm{Im}}^{+\,*} = \dfrac{259\omega\mu_0}{2000\pi} + \dfrac{\omega\mu_0}{2\pi} \ln\left(\dfrac{d_{ij} \cdot R_2}{R_1 \cdot R_3}\right) + \dfrac{8\omega\mu_0\left(R_3 - R_2\right)}{6\pi\left(R_3 + R_2\right)} - \dfrac{Y^3}{Y^2 + \left(\dfrac{\rho_S}{\pi\left(R_3^2 - R_2^2\right)}\right)^2} \\ Z_{\mathrm{Im}}^{+} = \dfrac{\sqrt{\omega\mu_0\rho_c}}{\sqrt{8}\pi R_1} + \dfrac{\omega\mu_0}{2\pi} \ln\left(\dfrac{d_{ij} \cdot R_2}{R_1 \cdot R_3}\right) + \dfrac{8\omega\mu_0\left(R_3 - R_2\right)}{6\pi\left(R_3 + R_2\right)} - \dfrac{Y^3}{Y^2 + \left(\dfrac{\rho_S}{\pi\left(R_3^2 - R_2^2\right)}\right)^2} \end{cases} \tag{11}$$

$$\text{where} \begin{cases} Z_{\mathrm{Im}}^{+\,*}, \text{ if } \sqrt{\dfrac{CS \cdot f}{\rho_c}} < 1725 \\ Z_{\mathrm{Im}}^{+}, \text{ if } \sqrt{\dfrac{CS \cdot f}{\rho_c}} \geq 1725 \end{cases}$$

B. Resistance

The resistance (12) is calculated substituting the variables in (8) by the equations from [1]. Alike the reactance, X is several times smaller than Y and (12) simplifies to (13).

$$Z_{\mathrm{Re}}^{+} = \frac{R_1\sqrt{\dfrac{\omega \cdot \mu_0 \cdot \rho_c}{8}} + \rho_c \dfrac{277}{777}}{\pi R_1^2} - \frac{\left(1.5X + Y\right)^2 \left(-\dfrac{\rho_S}{\pi\left(R_3^2 - R_2^2\right)}\right)}{\left(X + Y\right)^2 + \left(\dfrac{\rho_S}{\pi\left(R_3^2 - R_2^2\right)}\right)^2} \tag{12}$$

$$\begin{cases} Z_{\mathrm{Re}}^{+} = \dfrac{\rho_c}{\pi R_1^2} + \dfrac{Y^2\left(\dfrac{\rho_S}{\pi\left(R_3^2 - R_2^2\right)}\right)}{Y^2 + \left(\dfrac{\rho_S}{\pi\left(R_3^2 - R_2^2\right)}\right)^2}, \text{ if } \sqrt{\dfrac{CS \cdot f}{\rho_C}} < 1150 \\ Z_{\mathrm{Re}}^{+} = \dfrac{R_1\sqrt{\dfrac{\omega \cdot \mu_0 \cdot \rho_c}{8}} + \rho_c \dfrac{277}{777}}{\pi R_1^2} + \dfrac{Y^2\left(\dfrac{\rho_S}{\pi\left(R_3^2 - R_2^2\right)}\right)}{Y^2 + \left(\dfrac{\rho_S}{\pi\left(R_3^2 - R_2^2\right)}\right)^2}, \text{ if } \sqrt{\dfrac{CS \cdot f}{\rho_C}} \geq 1150 \end{cases} \tag{13}$$

C. Flat formations

The matrix (1) is different for cables installed in flat formation and some variables D have to be replaced by a new variable E. For a perfectly transposed cable D and E average and the final value is the same for both. Thus, (5) continues to be valid. The only change is the replacement in D of d_{ij} by the geometric mean distance [2]. A new expression for (5) can be developed for non-transposed cables, but it would complicate the calculations. Instead, the same expression is used. The sensitivity tests made in the next chapters validate this hypothesis and show that the error is negligible.

V. Validation

A. Sensitivity Tests

The equations are validated by comparing the reactance and resistance calculated using (11) and (13) against the reference formulae from [2], [3] and [4]. A series of sensitivity tests are prepared, where the eight parameters indicated in Table I are varied in equally spaced intervals 31 times. The variation is made individually for each parameter. Table I shows the minimum, maximum and reference values for each of the tested parameters.

TABLE I. MINIMUM, MAXIMUM AND REFERENCE VALUES USED IN THE SENSITIVITY ANALYSIS

	Min	Max	Reference
Conductor Resist. (ρ_c) [Ω.m]	$1\text{x}10^{-8}$	$4\text{x}10^{-8}$	$3.122\text{x}10^{-8}$
Screen Resist. (ρ_S) [Ω.m]	$1\text{x}10^{-8}$	$4\text{x}10^{-8}$	$1.72\text{x}10^{-8}$
Earth Resistivity (ρ_e) [Ω.m]	5	155	100
Conductor radius (R_1) [m]	$10\text{x}10^{-3}$	$40\text{x}10^{-3}$	$16.85\text{x}10^{-3}$
Insulation radius (R_2) [m]	$\text{R1}+10\text{x}10^{-3}$	$\text{R1}+40\text{x}10^{-3}$	$35.05\text{x}10^{-3}$
Screen radius (R_3) [m]	$\text{R2}+0.1\text{x}10^{-3}$	$\text{R2}+1.6\text{x}10^{-3}$	$35.479\text{x}10^{-3}$
Outer insul. radius (R_4) [m]	$\text{R3}+0.5\ \text{x}10^{-3}$	$\text{R3}+15.5\ \text{x}10^{-3}$	$41.5\ \text{x}10^{-3}$
Dist. flat form. (Dist) [m]	0.25	7.75	-

Fig. 1 and Fig. 2 show the error in percentage for the minimum and maximum values of the sensitivity test (Table I) for eight different frequencies between 1Hz and 10kHz. The value of the earth resistivity does not affect the results and it is not shown, instead the figures show the error for the reference cable. The figures only show two of the 31 tested cases. The errors of the other 29 are without exception between the two values shown in the figures. For a better visualisation the graphs are truncated and the error is presented numerically for some columns.

The relative error is small, typically inferior to 3% for the reactance and to 5% for the resistance. The exception is for large screens (R_3), which have large estimation errors. However, it is important to point out that the maximum R_3 value used in sensitivity tests is several times larger than the real value. I.e., it is likely that the errors are smaller for real cables, since that the individual change of the parameters leads to unrealistic cables. The next section addresses this issue.

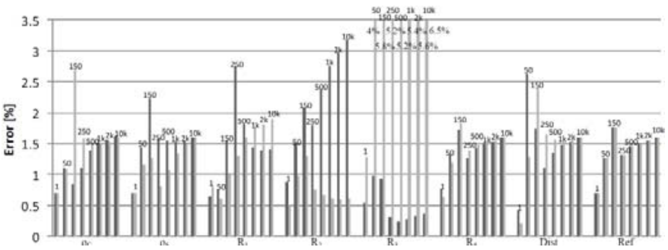

Fig. 1. Relative error of the reactance at different frequencies (indicated at the top of the columns) when using the proposed method for: different conductor (ρ_C) and screen (ρ_S) resistivities; different conductor (R_1), insulation (R_2), screen (R_3) and outer insulation (R_4) radiuses; different distance between cables when installed in flat formation (Dist). Dark columns: Min. value; Light columns: Max. value;

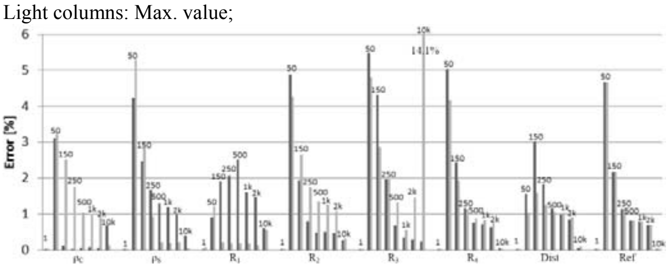

Fig. 2. Relative error of the resistance at different frequencies (indicated at the top of the columns) when using the proposed method for: different conductor (ρ_C) and screen (ρ_S) resistivities; different conductor (R_1), insulation (R_2), screen (R_3) and outer insulation (R_4) radiuses; different distance between cables when installed in flat formation (Dist). Dark columns: Min. value; Light columns: Max. value;

B. *Validation for generic cables*

The previous section tested the proposal formulae for a reference cable. Each parameter was changed individually over a large range of values and became eventually too big or too small when compared with the remaining parameters, resulting in unrealistic cables. As a result, some of the simulations have no real meaning, mainly those for the extreme of the test intervals, which also presented the largest errors. Thus, the accuracy of the formulae may be better than indicated in the previous section when applied to real cables.

This section tests the proposed formulae for different nominal voltage and cross-section areas, using data from the ABB [8] and Nexans [9] catalogues. Eighteen cables are tested, 9 from [8] and 9 from [9]. The cables from [8] have a copper conductor, whereas the cables from [9] have an aluminium conductor.

The correction of the resistivity, for stranded conductors, and of the permittivity, due to the semi-conductor layers [2], is not made. The objective is to compare calculation methods and thus, the correction is not important. The temperature of the conductor is 20°C, the ground resistivity is 100**Ω**.m and the top cable is installed at a depth of 1m. The error is estimated for ten different frequencies from 1Hz to 50kHz. The following cables are used in the comparison:

- 66kV: 120mm^2; 630mm^2 and 2000mm^2 [8]
- 150kV: 240mm^2; 1200mm^2 and 2500mm^2 [8]
- 400kV: 630mm^2; 1400mm^2 and 2500mm^2 [8]
- 66kV: 185mm^2; 500mm^2 and 1600mm^2 [9]
- 150kV: 400mm^2; 1000mm^2 and 2000mm^2 [9]
- 400kV: 500mm^2; 1200mm^2 and 3000mm^2 [9]

Fig. 3-Fig. 6 show the error in percentage of the proposed formulae for the cables installed in trefoil formation, whereas Fig. 7 and Fig. 8 show the estimated inductance and resistance in function of the frequency, using both the reference and the proposed formulae for the 66kV cables.

Formulae for the estimation of a cable's impedance at power frequency exist [2], [7]. One of the main objectives of this paper is to design formulae with a similar mathematical complexity, but accurate for more frequencies. Thus, the error obtained when using the power-frequency reference formulae is also presented in the figures and it can be seen that it is substantially large when compared with the proposed formulae. The results for flat formation are in Appendix and the values are similar to these.

The results confirm those of the previous section. The error for the reactance are typically very small, under 2% to all cable from [8] and below 2.5% for all cables from [9] with two exceptions, both for the 66kV cable from reference [9]. The error is larger for these two cables, because of the large cross-sections of the screen. As an example, the cross-section area of the screen of a 66kV-185mm^2 cable is 35mm^2 in reference [8] and 105mm^2 in reference [9]. Moreover, no information is given about the thickness of the semi-conductive layers in [9] and they are not considered in the simulations. Thus, the real thickness of the screen is smaller than the one used in this validation. As an example, the error at 50kHz of the cable with a screen cross-section area 105mm^2

would reduce from 5.8% to 4.2% if there was considered the presence of two semi-conductive layers with a thickness of 1mm.

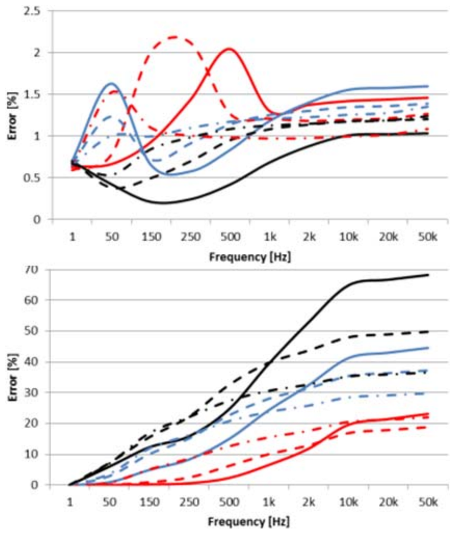

Fig. 3. Error in percent of the reactance for the proposed formulae (up) and the power-frequency formulae (down) for the cables reported in reference [8] installed in trefoil formation. Solid line: 66kV; Dashed line: 150kV; Dotted-dashed line: 400kV; Red: small cross-section; Blue: Medium cross-section; Black: Large cross-section

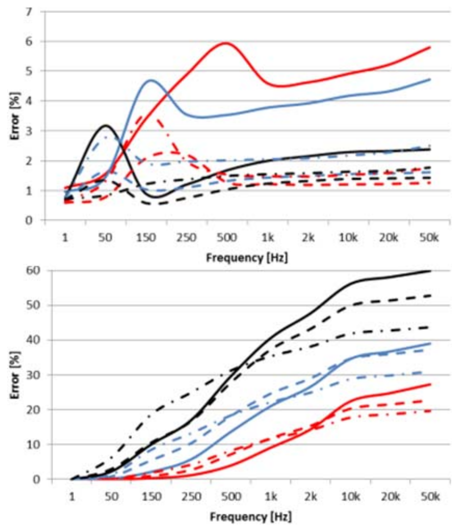

Fig. 4. Error in percent of the reactance for the proposed formulae (up) and the power-frequency formulae (down) for the cables reported in reference [9] installed in trefoil formation. Solid line: 66kV; Dashed line: 150kV; Dotted-dashed line: 400kV; Red: small cross-section; Blue: Medium cross-section; Black: Large cross-section

The error associated to the resistance is inferior to 4% for all cables up to 10kHz, becoming large for 20kHz and 50kHz. The error is positive up to 2kHz, meaning that the estimated resistance is larger than in the reference formulae and it becomes negative at 10kHz for the majority of the cables. This means that the proposed formulae are unable to accurately estimated the increase of the resistance due to skin and proximity effects for frequency larger than 10kHz. This result is expected as the simplifications made for the loop impedances were made for temporary overvoltages, slow-front overvoltages and resonances, phenomena with frequencies below 10kHz.

In summary, the comparisons show that the error is acceptable for the frequencies of interest. The reactance is accurately estimated for all frequencies and the resistance is accurately estimated up to 10kHz.

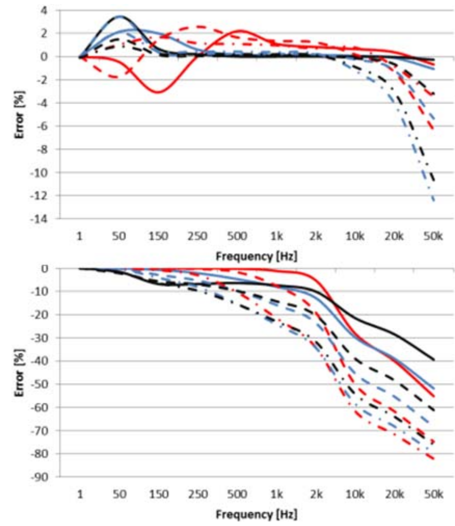

Fig. 5. Error in percent of the resistance for the proposed formulae (up) and the power-frequency formulae (down) for the cables reported in reference [8] installed in trefoil formation. Solid line: 66kV; Dashed line: 150kV; Dotted-dashed line: 400kV; Red: small cross-section; Blue: Medium cross-section; Black: Large cross-section

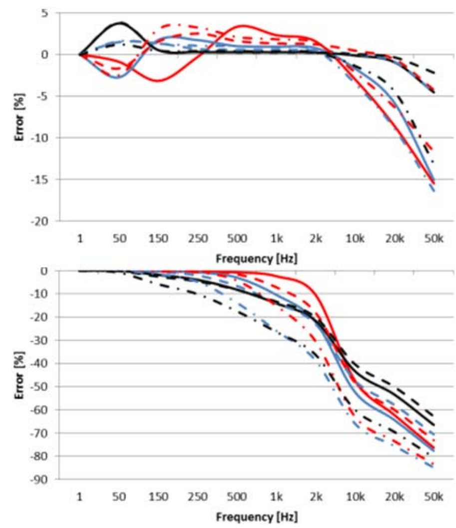

Fig. 6. Error in percent of the resistance for the proposed formulae (up) and the power-frequency formulae (down) for the cables reported in reference [9] installed in trefoil formation. Solid line: 66kV; Dashed line: 150kV; Dotted-dashed line: 400kV; Red: small cross-section; Blue: Medium cross-section; Black: Large cross-section

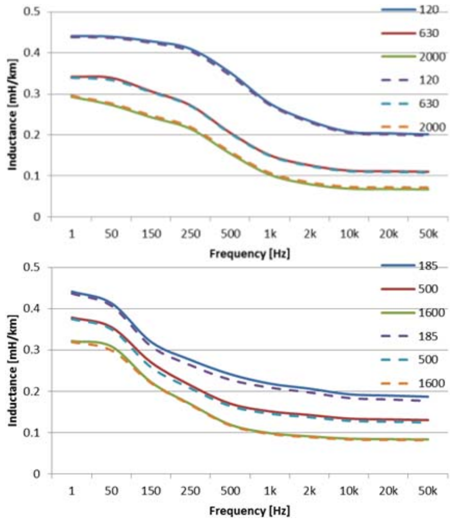

Fig. 7. Inductance of the different cross-sections of proposed (solid lines) and reference (dashed lines) formulae for the 66kV cables reported in [8] (up) and [9] (down) in trefoil formation

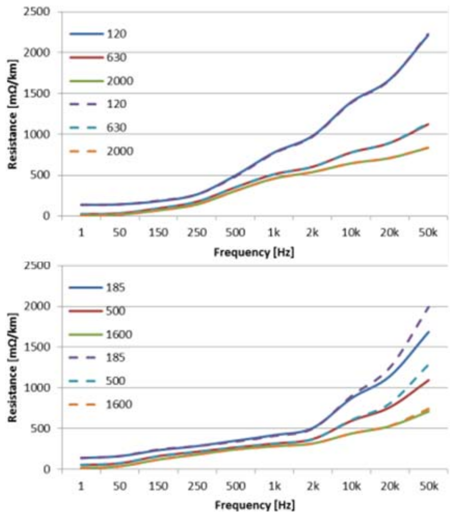

Fig. 8. Resistance of the different cross-sections of proposed (solid lines) and reference (dashed lines) formulae for the 66kV cables reported in [8] (up) and [9] (down) in trefoil formation

VI. Resonance Calculations

The proposed formulae can be used to estimate the resonance frequency of a cable during its energisation, a task often done with software help that requires building a model of the network. Reference [5] presents a method that can be used to estimate the resonance frequency using the reference formulae and it is, therefore, more exact, but also more complex than the method proposed in this paper.

The resonance frequency associated to the energisation of a cable is given by (14).

$$f = \frac{1}{4l\sqrt{C_{ap}\cdot\left(L(f)+\left(\frac{2\pi}{4}\right)^2\cdot\frac{L_{eq}}{l}\right)}} \tag{14}$$

The resonance frequency of the energisation is calculated using equations (11) and (14) in an iterative process. The inductance $L(f)$ in (14) is first calculated for 50Hz, or other random frequency, using (11) and a new frequency is calculated using (14). The inductance is recalculated for the new frequency and the process repeats itself until the values no longer change.

Fig. 9 compares the resonance frequencies estimated using this process versus simulations in PSCAD, for four different cables and five short-circuit powers. The first cable is a 400kV-40km cable, the second is a 150kV-20km cable, the third is a 400kV-5km cable and the last is a 20kV-5km cable. The estimation is accurate for all four cases and the error is inferior to 2% to nearly all short-circuit powers. Moreover, part of the error is not associated to the calculation of the inductance, but to (14), which does not considered the distributed nature of a cable's impedance.

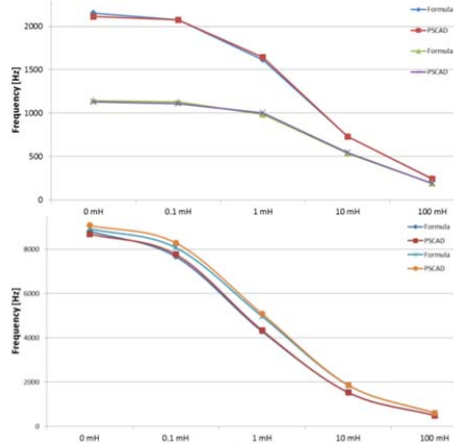

Fig. 9. Resonance frequency for different short-circuit power levels. Left - Upper lines: 150kV-20km cable; Bottom lines: 400kV-40km cable; Right: Upper lines: 20kV-5km cable; Bottom lines: 150kV-5km cable;

The resonance frequency is also estimated using the power frequency formulae in order to compare their accuracy with the accuracy of the formulae proposed in this paper.

Fig. 10 shows the error of the two when compared with the PSCAD simulations. The results show that the error is substantially lower when using the proposed formulae than the power frequency formulae. The low error for low short-circuit powers is explained by the dominance of the equivalent network's inductance.

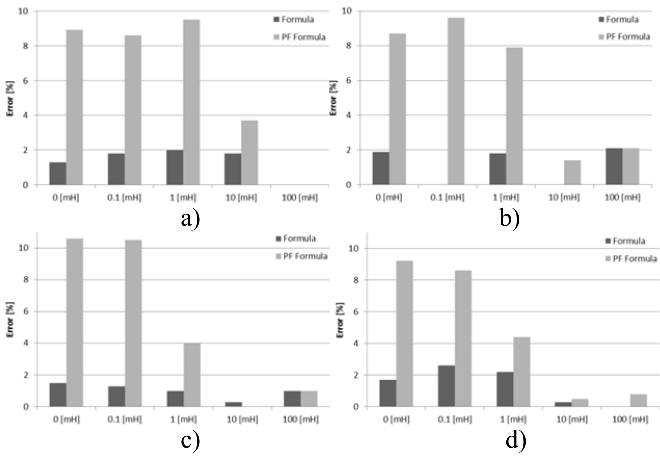

Fig. 10. Error in percent when estimating the resonance frequency using the formulae proposed in this paper (dark columns) and the formulae used for calculations at power frequency (light columns). a) 400kV – 40km; b) 150kV – 20km; c) 150kV – 5km; d) 20kV – 5km

VII. Advantages and Disadvantages

The development of new formulae for the calculation of the positive-sequence impedance of three-phase single-core cables and the respective validation were made in the previous chapters. The discussion of the advantages and disadvantages of these formulae is relevant to show that in some situations it is beneficial to use them in substitution of the existing ones.

Advantages of the formulae:

- do not require several steps or the use of mathematical software;
- the mathematical complexity is at the same level of the formulae used for calculating the impedance of a cable at power frequency, with the advantage of being accurate over a large range of frequencies;
- the results are accurate for frequencies associated to temporary overvoltages, slow-front overvoltages and resonances;
- provide a fast estimation of the resonance frequency, which can be used to set up the target frequency of a Bergeron model or to verify the triggering of temporary overvoltages, for example;

Disadvantages of the formulae:

- are still long and difficult to solve in one step using a calculator, but can be subdivided into parcels that can be added and multiplied; the same issue exits for the standard formulae used for estimating the two parameters at power-frequency;
- have to be corrected for low frequencies and/or small cross-sections, introducing more complexity; however, this correction is not expected for the majority of real cases;
- do not calculate zero-sequence impedance;

In summary, the formulae are useful for cases that require the calculation of the positive-sequence impedance of a cable. They are less complex, easy to implement, can save time and reduce lapses.

Studies that require information on the modal velocities, modal attenuations or zero-sequence impedance should continue to use the reference formulae.

VIII. Conclusions

This paper presented new simplified formulae that can be used in the estimation of the positive-sequence resistance and reactance of three-phase single-core cables for the frequencies associated to typical electromagnetic transients and resonance phenomena.

The formulae were validated for different voltage levels and cross-sections, together with sensitivity tests. The accuracy of the simplified formulae is high and they can be used with a high degree of confidence in the estimation of the resistance and/or reactance of an underground cable.

IX. References

[1] F. Faria da Silva, "Simplified frequency-dependent formulae for series-impedance matrices of single-core HVAC cables", UPEC 2015

[2] CIGRE WG B1.30, "Cable Systems Electrical Characteristics", 2013

[3] L. M. Wedepohl, D. J. Wilcox, "Transient analysis of underground power-transmission systems: System-model and wave-propagation characteristics", Proceedings of the Institution of Electrical Engineers, Vol. 120, No. 2, 1973

[4] A. Ametani, "A General Formulation of Impedance and Admittance of Cables", IEEE Transactions on Power Apparatus and Systems, 1980

[5] Teruo Ohno, Claus Leth Bak, Ametani Akihiro, Wojciech Wiechowski, Thomas K. Sørensen, "Derivation of Theoretical Formulas of the Frequency Component Contained in the Overvoltage related to Long EHV Cables", IEEE Transactions on Power Delivery, 2012

[6] Nassler Tleis, "Power Systems Modelling and Fault Analysis", Elsevier-Newnes, 2008

[7] CIGRE WG C4.502, "Power System Technical Performance Issues Related to the Application of Long HVAC Cables", October 2013

[8] ABB, "XLPE Land Cable Systems – User's Guide", Rev 5, 2010

[9] Nexans,"60-500kV High Voltage Underground Power Cables–XLPE insulated cables", Ed. 10, 2011

X. Appendix

A. Error Flat Formation

Fig. 11 shows the error of the proposed formulae for cables installed in flat formation, with 1m separation. The error associated to flat formations is in the same range of the error associated to trefoil formations and the explanation of the results is the alike the one provided in the paper to the latter. The results also show that non-transposed flat cables can be considered as perfectly transposed without affecting the accuracy.

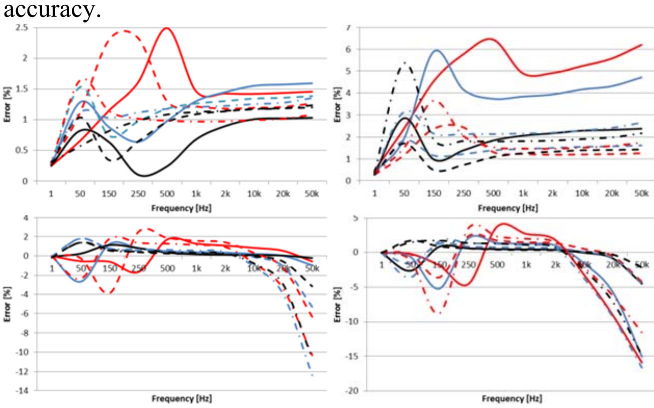

Fig. 11. Error in percent of reactance (up) and resistance (down) for the proposed formulae for the cables from [8] (left) and [9] (right) in flat formation. Solid line: 66kV; Dashed line: 150kV; Dotted-dashed line: 400kV; Cross-sections: Red: small; Blue: Medium; Black: Large